Cell Reports

Report

Regulation of Nucleosome Architecture and Factor Binding Revealed by Nuclease Footprinting of the ESC Genome

Graphical Abstract

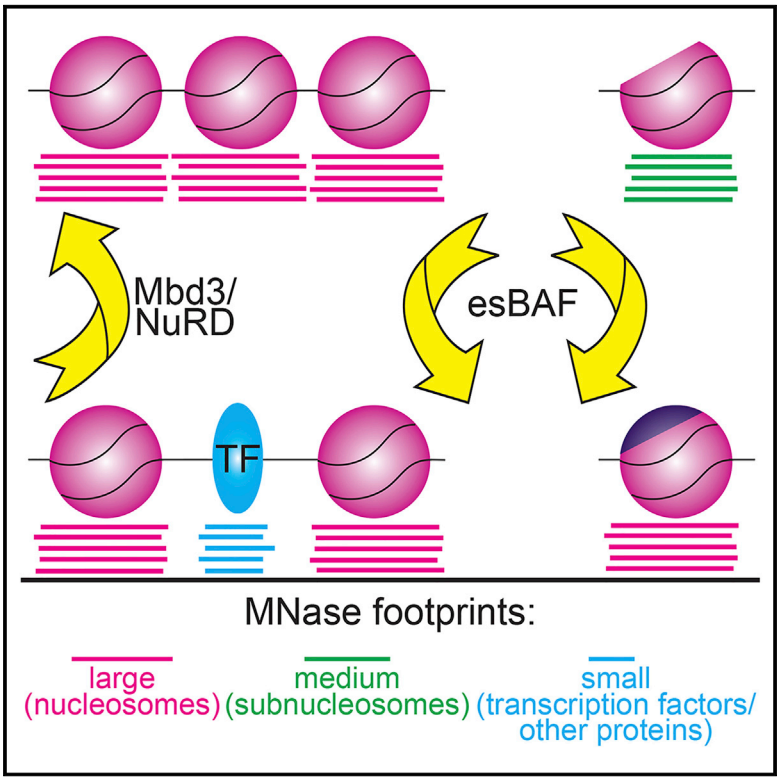

Authors

Sarah J. Hainer, Thomas G. Fazzio

Correspondence

thomas.fazzio@umassmed.edu

In Brief

Functional connections among chromatin regulators and factors that control gene-regulatory networks are often elusive. Hainer and Fazzio use nuclease footprinting in embryonic stem cells to uncover functions of two chromatin-remodeling complexes in regulatory factor binding and intra-nucleosome architecture.

Highlights

- Alterations in MNase footprints reveal functional interactions among gene regulators
- esBAF and Mbd3/NuRD regulate the occupancy of multiple regulatory proteins in ESCs
- esBAF is required for Klf4 binding in ESCs
- esBAF functions in subnucleosome maturation through regulation of H2A.Z occupancy

Accession Numbers

GSE68400

Hainer & Fazzio, 2015, Cell Reports *13*, 61–69
October 6, 2015
http://dx.doi.org/10.1016/j.celrep.2015.08.071

CellPress

Cell Reports
Report

Regulation of Nucleosome Architecture and Factor Binding Revealed by Nuclease Footprinting of the ESC Genome

Sarah J. Hainer[1,2] and Thomas G. Fazzio[1,2,*]
[1]Department of Molecular, Cell, and Cancer Biology, University of Massachusetts Medical School, Worcester, MA 01605, USA
[2]Program in Molecular Medicine, University of Massachusetts Medical School, Worcester, MA 01605, USA
*Correspondence: thomas.fazzio@umassmed.edu
http://dx.doi.org/10.1016/j.celrep.2015.08.071

SUMMARY

Functional interactions between gene regulatory factors and chromatin architecture have been difficult to directly assess. Here, we use micrococcal nuclease (MNase) footprinting to probe the functions of two chromatin-remodeling complexes. By simultaneously quantifying alterations in small MNase footprints over the binding sites of 30 regulatory factors in mouse embryonic stem cells (ESCs), we provide evidence that esBAF and Mbd3/NuRD modulate the binding of several regulatory proteins. In addition, we find that nucleosome occupancy is reduced at specific loci in favor of subnucleosomes upon depletion of esBAF, including sites of histone H2A.Z localization. Consistent with these data, we demonstrate that esBAF is required for normal H2A.Z localization in ESCs, suggesting esBAF either stabilizes H2A.Z-containing nucleosomes or promotes subnucleosome to nucleosome conversion by facilitating H2A.Z deposition. Therefore, integrative examination of MNase footprints reveals insights into nucleosome dynamics and functional interactions between chromatin structure and key gene-regulatory factors.

INTRODUCTION

In eukaryotes, genomic DNA is packaged with proteins to form chromatin: a repeating array of nucleosomes that each contain 147 bp of DNA wrapped around an octamer of histone proteins composed of a tetramer of H3 and H4 and two H2A and H2B heterodimers (Luger et al., 1997). In some cases, these canonical histone proteins can be replaced with histone variants (such as H2A.Z or H3.3), which contain high sequence similarity to their canonical counterparts but have somewhat specialized functions in vivo. Regulation of access to factor binding sites through alteration of nucleosome occupancy or positioning is an important mechanism shared among eukaryotes (Almer and Hörz, 1986; Boeger et al., 2003). As a result, most eukaryotic regulatory regions are found within nucleosome-depleted regions, which permit binding of regulatory factors and transcription machinery (Mavrich et al., 2008a; Weiner et al., 2010; Yuan et al., 2005).

Nucleosome-remodeling factors reposition, deposit, or remove nucleosomes at regulatory regions by altering histone-DNA contacts (Bartholomew, 2014; Racki and Narlikar, 2008). esBAF (Brg1-associated factor) is an embryonic stem cell (ESC)-specific nucleosome-remodeling complex that mainly activates transcription of genes and silences transcription near enhancers (Hainer et al., 2015; Ho et al., 2009a, 2009b, 2011) and is necessary for ESC self-renewal and pluripotency (Fazzio et al., 2008; Ho et al., 2009a; Kidder et al., 2009; Schaniel et al., 2009). The Mbd3/NuRD (nucleosome remodeling and deacetylase) complex creates repressive chromatin structure and is required for normal ESC differentiation (Denslow and Wade, 2007; Kaji et al., 2006, 2007; Yildirim et al., 2011). Interestingly, esBAF and Mbd3/NuRD antagonistically regulate many overlapping gene targets, resulting in moderate levels of expression (Yildirim et al., 2011).

Although nucleosome positioning and occupancy have been examined in multiple systems (Carone et al., 2014; Li et al., 2012; Mavrich et al., 2008b; Schones et al., 2008; Valouev et al., 2011), very little is known about the regulation of subnucleosomes—histone-DNA structures that lack some components of the histone octamer. Hexasomes (one H3/H4 tetramer and one H2A/H2B dimer) and half-nucleosomes (either an H3/H4 tetramer or half an H3/H4 tetramer and one H2A/H2B dimer) have been observed in vivo (Rhee et al., 2014). However, the conditions under which subnucleosomes form, the mechanisms underlying their assembly, and the roles of nucleosome-remodeling factors in regulating interchange of subnucleosome and nucleosome structures are largely unknown.

Here, we take an integrative approach to survey the functions of two chromatin-remodeling complexes with key roles in ESC pluripotency, utilizing micrococcal nuclease (MNase) footprinting to reveal nucleosome footprints (135–165 bp), subnucleosome footprints (100–130 bp), and footprints of regulatory factors ($\leq$80 bp), as previously described (Carone et al., 2014; Henikoff et al., 2011; Kent et al., 2011). Using this method, we analyzed the chromatin structure of ESCs depleted of important factors to determine their roles in controlling nucleosome and subnucleosome architecture, as well as regulatory factor occupancy. We provide evidence that esBAF and Mbd3/NuRD modulate the binding of several regulatory factors, and we

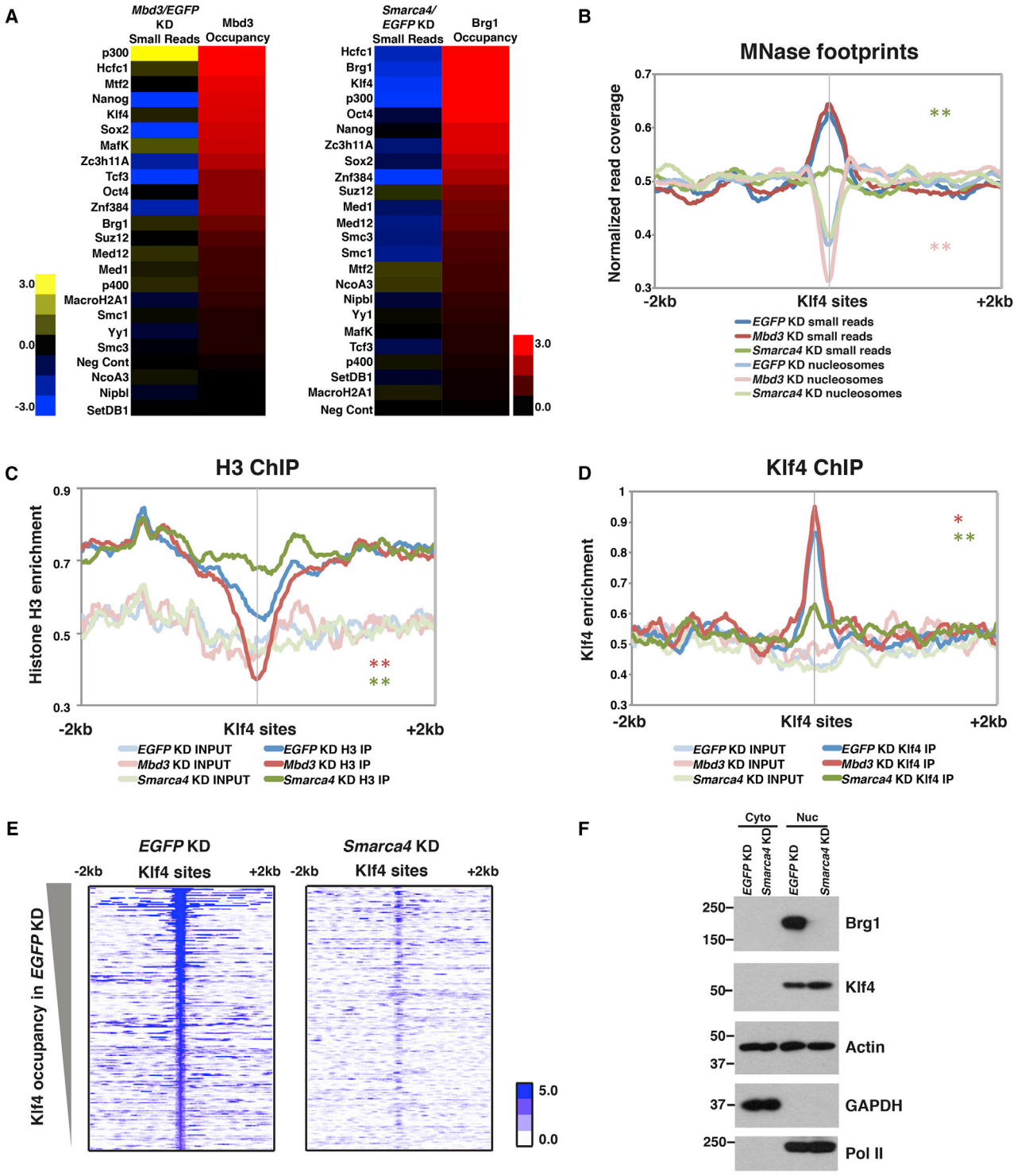

Figure 1. Klf4 Binding Is esBAF-Dependent

(A) Log_2 fold change of small read footprints (left: *Mbd3/EGFP* KD; right: *Smarca4/EGFP* KD) spanning 200 bp directly over binding peaks sorted by either Mbd3 (left) or Brg1 (right) occupancy.

(B) Aggregation plot of normalized small reads ($\leq$80 bp) and nucleosome size reads (135–165 bp) of MNase-seq upon *EGFP*, *Mbd3*, or *Smarca4* KD over Klf4 binding sites. Klf4 binding sites were called from GEO: GSE11431 (Chen et al., 2008). Asterisks (* and **) indicate p values (<0.05; <0.01), reflecting statistical significance of changes in MNase footprints over the relative to *EGFP* KD, colored as indicated in key.

(C) Histone H3 ChIP-seq in *EGFP*, *Mbd3*, or *Smarca4* KD ESCs shown as normalized occupancy aggregated over Klf4 binding sites.

(legend continued on next page)

specifically demonstrate that esBAF is required for Klf4 occupancy in ESCs. Furthermore, we find that in the absence of esBAF, the abundance of subnucleosomes is increased at the expense of nucleosomes at specific loci, most notably at sites of H2A.Z localization. Consistent with these results, we find that H2A.Z occupancy is strongly decreased in the absence of esBAF. These data suggest esBAF promotes nucleosome occupancy by stabilizing H2A.Z-containing nucleosomes (to prevent conversion of nucleosomes into subnucleosomes) or promoting H2A.Z deposition, potentially by facilitating the functions of H2A.Z deposition factors.

These findings reveal that, by quantifying changes in the abundance of MNase footprints, one can quickly and easily uncover interactions between chromatin-remodeling proteins and gene-regulatory factors, which can subsequently be validated by standard approaches. Furthermore, changes in subnucleosome size footprints relative to nucleosome footprints provide insights into the regulation of intra-nucleosome architecture, which have been elusive. Therefore, MNase footprinting is a powerful tool for the study of chromatin dynamics in living cells.

RESULTS AND DISCUSSION

Alterations in Footprinting of Multiple Regulatory Proteins upon Loss of esBAF or Mbd3/NuRD Function

Previously, we used deep sequencing of DNA footprints protected from MNase digestion to map nucleosomes in ESCs depleted of esBAF and Mbd3/NuRD (Hainer et al., 2015). To test the roles of these complexes in regulation of transcription factor and chromatin regulatory factor binding, we focused on the information provided by the small reads ($\leq$80 bp) obtained from these MNase-seq experiments. Proof-of-concept analyses have been performed in yeast and mammalian cells, showing that peaks of small MNase footprints correspond to binding sites for factors determined by independent methods, such as ChIP-seq (Carone et al., 2014; Henikoff et al., 2011; Kent et al., 2011). Therefore, we plotted the average abundance of small read footprints ($\leq$80 bp) from *EGFP*, *Mbd3*, and *Smarca4* KD ESCs that mapped to 32 distinct genomic regions: the experimentally determined binding sites of 30 key components of the ESC gene regulatory network (including Brg1 itself, as a positive control), annotated transcription start sites (TSSs), and a random selection of nucleosome-bound regions as a negative control (Figure S1; Data S1A).

We performed several analyses to assess data quality. First, we quantified changes in small read footprints directly over the factor binding sites and used available ChIP-seq data for Mbd3 and Brg1 to distinguish changes in factor occupancy directly due to loss of Mbd3/NuRD or esBAF function (Figure 1A). For both esBAF and Mbd3/NuRD, we observed minimal alterations in footprinting at factor binding sites at which Brg1 and Mbd3 were not highly enriched (Figure 1A). As a positive control, small read footprints were dramatically changed at the empirically determined binding sites of Brg1 upon *Smarca4* KD. Finally, as a negative control, we observed no changes in small reads over a random sampling of nucleosomes, demonstrating alterations in esBAF and Mbd3/NuRD are confined to specific regions of the genome.

Smarca4 KD resulted in a substantial reduction in small read accumulation at several sites (Figure 1A; Data S1A), consistent with the function of esBAF to create open chromatin structure to facilitate binding of regulatory factors and the general transcription machinery (Ho et al., 2009a, 2009b, 2011; Novershtern and Hanna, 2011; Yildirim et al., 2011). Whereas KD of *Mbd3* resulted in subtle changes in MNase footprinting at most sites relative to *Smarca4* KD, we observed a strong increase in peaks of small reads at p300 binding sites in *Mbd3* KD cells, consistent with the antagonistic roles of Mbd3/NuRD and p300 in enhancer function (Pasini et al., 2010; Reynolds et al., 2012). Therefore, alterations in small read profiles from MNase-seq data suggest that both esBAF and Mbd3/NuRD are important regulators of transcription factor and chromatin regulatory factor binding.

esBAF Is Required for Klf4 Binding

Although alterations in small read profiles at transcription factor binding sites imply altered binding of transcription factors themselves, these changes could alternatively result from altered binding of cofactors that co-occupy the same binding sites or loss of esBAF or Mbd3/NuRD footprints when these factors are knocked down. To distinguish between these possibilities, we tested one functional interaction by an independent method. One of the factors that appeared most strongly affected by *Smarca4* KD was Klf4—small MNase footprints over Klf4 binding sites were strongly reduced upon *Smarca4* KD, whereas *Mbd3* KD had a very modest increase (Figures 1A and 1B). Klf4 plays a critical role in maintenance of the ESC gene-regulatory network (Kim et al., 2012; Schuh et al., 1986; Takahashi and Yamanaka, 2006), and Klf4 binding sites are highly bound by Brg1, consistent with the possibility that esBAF promotes Klf4 binding (Figure 1A).

When we examined the nucleosome size (135–165 bp) MNase footprints over Klf4 binding sites, we observed a small increase in nucleosome footprints upon *Smarca4* KD (Figure 1B), suggesting that esBAF may promote Klf4 binding in part by clearing its binding sites of nucleosomes. To test this prediction, we performed ChIP-seq for histone H3 and Klf4 in *EGFP*, *Mbd3*, and *Smarca4* KD ESCs. Consistent with our MNase footprinting data, we observed increased histone H3 occupancy over Klf4 binding sites upon *Smarca4* KD and decreased histone H3 occupancy upon *Mbd3* KD (Figure 1C). These data are consistent with changes we observed in nucleosome size footprints at Klf4 binding sites and demonstrate that esBAF is required to maintain open chromatin structure over these regions. Furthermore,

(D) Klf4 ChIP-seq in *EGFP*, *Mbd3*, or *Smarca4* KD ESCs shown as normalized Klf4 occupancy aggregated over Klf4 binding sites.
(E) Heatmaps of Klf4 occupancy over Klf4 binding sites in *EGFP* (left) and *Smarca4* (right) KD. Occupancy is indicated as $\log_2$ (normalized reads).
(F) Equal levels of nuclear Klf4 in *EGFP* and *Smarca4* KD ESCs confirmed by western blotting. GAPDH and Pol II are specificity controls for cytoplasmic and nuclear fractions, respectively.

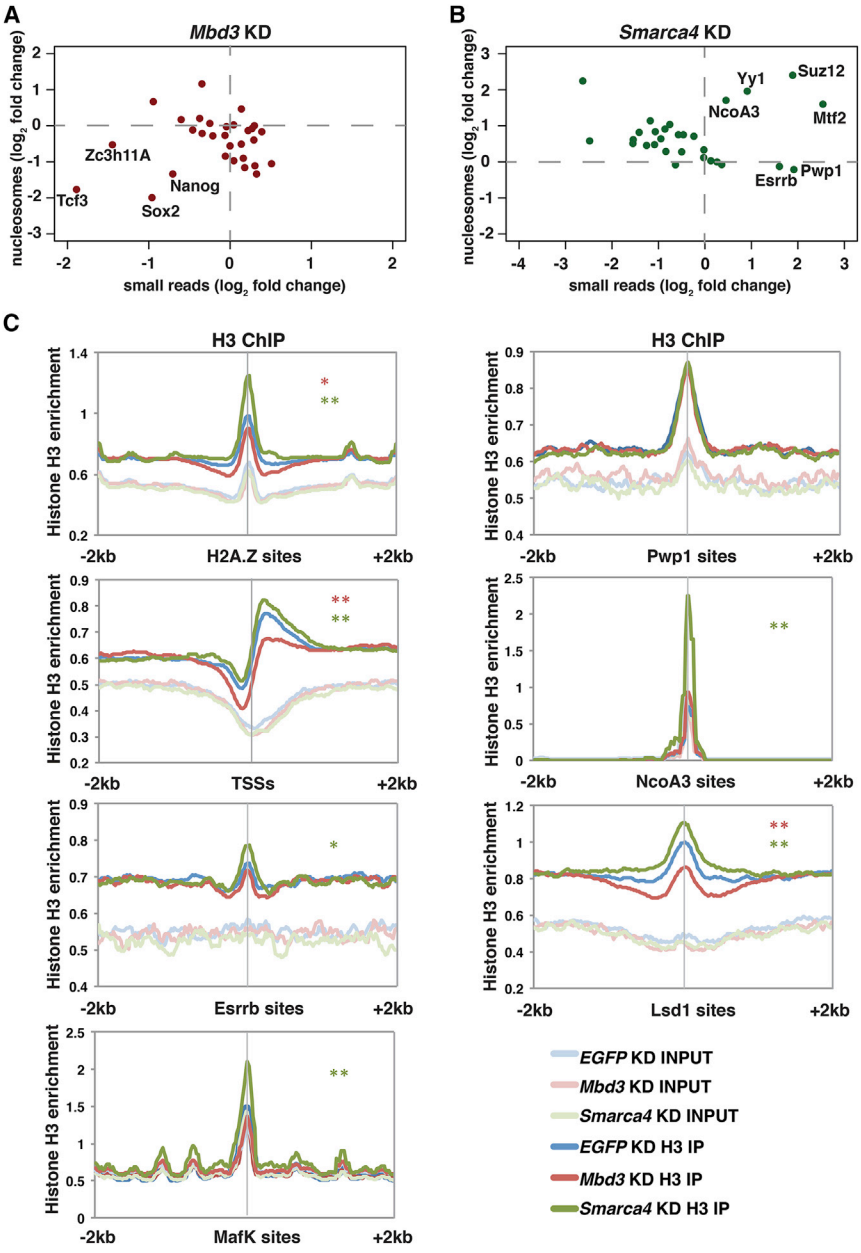

Figure 2. esBAF and Mbd3/NuRD Complexes Regulate Nucleosome Occupancy over Factor Binding Sites

(A and B) Scatterplot of $\log_2$ fold change values of nucleosome size reads versus small reads in *Mbd3* (A) or *Smarca4* (B) KD ESCs relative to *EGFP* KD. (C) Aggregation plots of histone H3 ChIP-seq over a subset of factor binding sites of *EGFP*, *Mbd3*, and *Smarca4* KD ESCs. Asterisks (* and **) indicate p values as described in Figure 1.

ChIP-seq of Klf4 showed a dramatic reduction in Klf4 occupancy over Klf4 binding sites in *Smarca4* KD cells and a slight increase in *Mbd3* KD cells (Figures 1D and 1E), demonstrating that alterations in small read abundance over Klf4 binding sites upon *Smarca4* and *Mbd3* KD directly reflect alterations in Klf4 binding. Depletion of Brg1 does not result in reduced levels or altered intracellular localization of Klf4, ruling out these potential indirect effects on Klf4 binding (Figure 1F).

We conclude that esBAF functions directly to promote Klf4 occupancy by maintaining open chromatin structure over Klf4 binding sites. These findings confirm that changes in small read profiles from MNase-seq experiments can uncover alterations in factor occupancies when mapped over experimentally determined peaks from ChIP-seq data sets. Future studies following up additional functional interactions predicted by these data should provide additional insights into the ESC gene-regulatory network.

esBAF and Mbd3/NuRD Regulate Factor Binding by Modulating Nucleosome Occupancy over Factor Binding Sites

We previously found that esBAF activates expression of many genes by reducing promoter-proximal nucleosome occupancy and facilitating binding of RNA polymerase II (RNAPII), whereas Mbd3/NuRD acts oppositely (Hainer et al., 2015; Yildirim et al., 2011). To test whether these complexes modulate binding of regulatory proteins by similar mechanisms, we examined the effect of *Smarca4* or *Mbd3* KD on the abundance of nucleosome footprints at regulatory factor binding sites (many of which are far from promoters). Because nucleosome occupancy often inhibits binding of regulatory proteins, we plotted the changes in small read footprints versus nucleosome footprints in *Mbd3* (Figure 2A) or *Smarca4* (Figure 2B) KD cells, relative to control, for all 30 sets of binding sites.

Similar to promoters, *Mbd3* KD resulted in decreased and *Smarca4* KD resulted in increased average abundance of nucleosome footprints at the binding sites of most factors (Figures 2A and 2B; compare points above and below horizontal lines). Also consistent with the requirement of most regulatory proteins for a nucleosome-free binding site, changes in the abundance of small read footprints anti-correlated with changes in nucleosome size footprints (Figures 2A and 2B). These data indicate that esBAF promotes factor binding by creating open chromatin structure and Mbd3/NuRD inhibits factor binding by creating a closed chromatin environment, consistent with the known biological functions of these factors (Ho et al., 2011; Novershtern and Hanna, 2011; Reynolds et al., 2012; Yildirim et al., 2011).

Although nucleosome footprints negatively correlate with small read footprints overall, there are exceptions at several

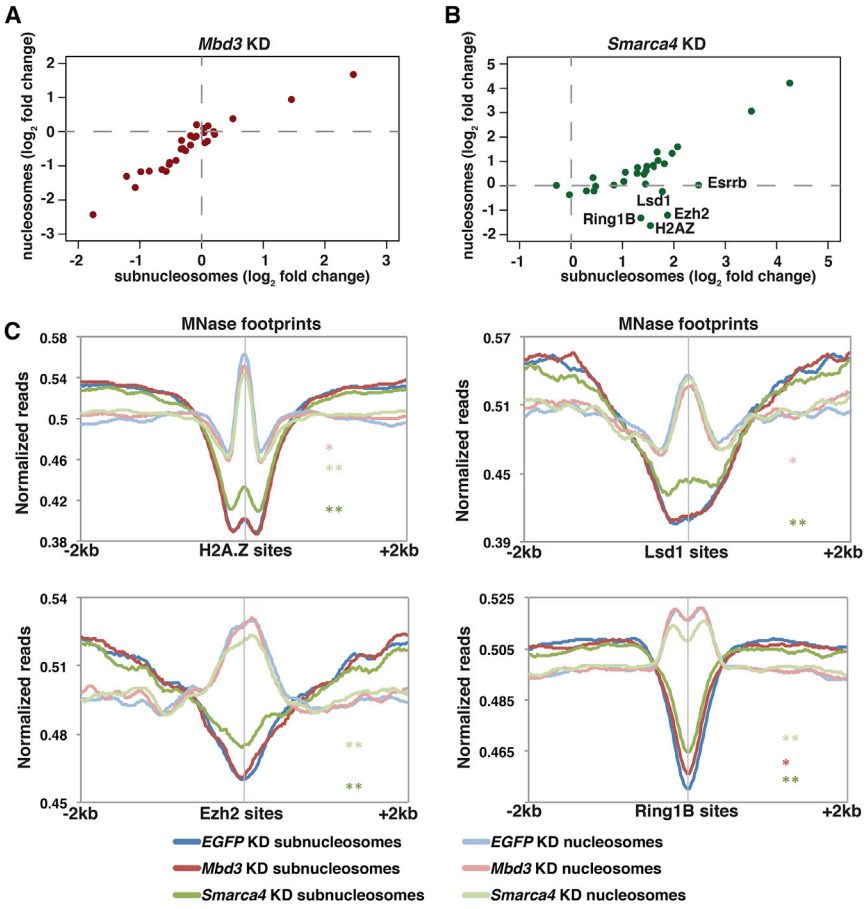

Figure 3. esBAF Promotes Nucleosome Formation at the Expense of Subnucleosomes

(A and B) Scatterplot of $\log_2$ fold change values of nucleosome size reads versus medium size reads in *Mbd3* (A) or *Smarca4* (B) KD ESCs relative to control ESCs.

(C) Aggregation plots of relative nucleosome (135–165 bp) and subnucleosome (100–130 bp) occupancy of MNase-seq data upon *EGFP*, *Mbd3*, or *Smarca4* KD over various factor binding sites. Asterisks (* and **) indicate p values as described in Figure 1.

locations (compare Data S1A and S1B), suggesting that nucleosome occupancy does not inhibit the binding of some factors (Figures 2A and 2B). At many of these sites, there are clear peaks of nucleosome size footprints centered on factor binding sites (Data S1B), consistent with this model. Importantly, the presence of nucleosomes over several of these sites is predicted by their functions. PRC2 binds and methylates histone H3K27 within nucleosomes (Margueron and Reinberg, 2011; Simon and Kingston, 2009), consistent with the co-localization of its Suz12, Ezh2, and Mtf2 subunits (Zhang et al., 2011) with nucleosome footprints. Similarly, Pwp1 (a WD40-repeat-containing protein) occupies regions marked with H4K20me3 and regulates H4K20 methylation at some sites (Shen et al., 2015) and Ring1b (an E3 ubiquitin ligase within PRC1 complexes) monoubiquitinates H2AK119 (Wang et al., 2004). Furthermore, Lsd1 is a histone H3 lysine demethylase (Shi et al., 2004). Finally, Esrrb has been shown to bind within regions occupied by nucleosomes (Teif et al., 2012), and NcoA3 interacts with Esrrb, co-occupying some locations on chromatin (Percharde et al., 2012).

To validate these findings, we analyzed our histone H3 ChIP-seq data in control, *Mbd3*, and *Smarca4* KD cells over a subset of factor binding sites (Figure 2C). As positive controls, we found that sites of H2A.Z incorporation have peaks of histone H3, whereas TSSs are depleted of histone H3 immediately upstream of the TSS and have strong peaks of occupancy over the +1 nucleosome location (Figure 2C). Consistent with our MNase footprinting data, we observed a strong peak of histone H3 occupancy over factor binding sites found to have nucleosome size MNase footprints, demonstrating that these sites are indeed occupied by nucleosomes (Figure 2C).

For one factor examined, the role of nucleosome architecture in regulating factor binding has not been addressed. MafK is a leucine zipper transcription factor that, to our knowledge, has not been shown to bind nucleosomes. Here, we found a peak of nucleosome size reads over MafK sites, and our histone H3 ChIP-seq data support these findings, suggesting that MafK binds DNA within nucleosome-occupied regions. Together, these data confirm that, although most regulatory factors bind to nucleosome-depleted regions of the genome, some do not. In addition, these data suggest that differential affinities of factors for nucleosome-bound DNA must be taken into account in studies examining their biochemical functions and roles within gene-regulatory networks.

esBAF Regulates Nucleosome-Subnucleosome Interconversion at Specific Sites

To globally address whether and how Mbd3/NuRD and esBAF regulate the composition of nucleosomes in ESCs, we compared nucleosome footprints (135–165 bp; Data S1B) to intermediate size footprints (100–130 bp; Data S1C) over the same factor sites. The intermediate size fragments could result from either large non-histone protein complexes or non-standard nucleosomes (i.e., hexasomes or half-nucleosomes). Consistent with the latter possibility, the profiles of nucleosome and intermediate size footprints (hereafter, subnucleosomes) were strongly positively correlated in both *Mbd3* and *Smarca4* KD cells (Figures 3A and 3B).

Interestingly, although subnucleosomes and nucleosomes were strongly correlated at all regions examined upon *Mbd3* KD (Figure 3A), KD of *Smarca4* resulted in alterations to subnucleosome footprints that were uncoupled from alterations in

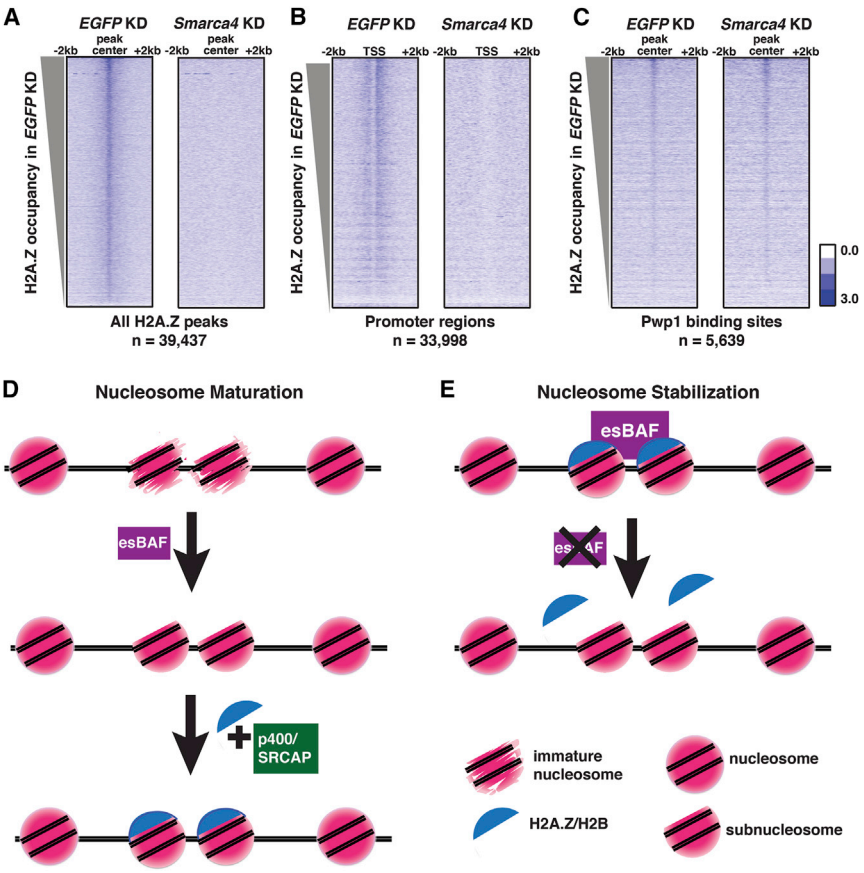

Figure 4. Brg1 Is Required for H2A.Z Occupancy at a Subset of Locations

(A–C) Heatmaps of H2A.Z occupancy over indicated regions in *EGFP* (left) and *Smarca4* (right) KD. Binding sites were taken from the following data sets: H2A.Z (GEO: GSE34483); TSSs (mm9); and Pwp1 (GEO: GSE59389). Occupancy is indicated as $\log_2$ (normalized reads).

(D) Maturation model of subnucleosome-nucleosome transition by esBAF. esBAF is required for converting subnucleosomes into a form suitable for H2A.Z/H2B incorporation by p400 or SRCAP, potentially by organizing wrapping of DNA around the H3/H4 tetramer, promoting accessibility of H3/H4 binding interfaces, or another mechanism.

(E) Stabilization model of subnucleosome regulation by esBAF. esBAF prevents disassembly of nucleosomes into subnucleosomes (such as hexasomes or half-nucleosomes) by preventing loss of H2A.Z/H2B or H2A/H2B dimers from the histone octamer. Maturation and stabilization of subnucleosomes could be occurring simultaneously, and esBAF could regulate H2A.Z occupancy based on interactions with additional regulatory factors.

nucleosome footprints at some sites (Figure 3B). At four locations where *Smarca4* KD results in either decreased (Ezh2, Ring1B, and H2A.Z sites) or had no effect on (Lsd1 sites) nucleosome occupancy, subnucleosome footprints are increased (Figure 3C). Importantly, histone H3 occupancy measured by ChIP-seq (which likely cannot discriminate between nucleosomes and subnucleosomes) is increased over Lsd1, Ezh2, Ring1B, and H2A.Z binding sites upon *Smarca4* KD (Figures 2C and S3), confirming that subnucleosome footprints at these sites reflect the presence of histones. Taken together, these data show that *Smarca4* KD results in higher subnucleosome occupancy and reduced nucleosome occupancy at a subset of genomic locations, suggesting esBAF is necessary for either maturation of subnucleosomes to nucleosomes or prevention of nucleosome disassembly at these sites.

Brg1 Is Required for Normal H2A.Z Localization

Whereas the mechanisms underlying subnucleosome-nucleosome interconversion are unknown, prior reports suggest that hexasomes are composed of an H3/H4 tetramer and a single H2A/H2B dimer (Rhee et al., 2014; Weintraub et al., 1975). These findings suggest that regulation of H2A/H2B (or H2A variant/H2B) dimer incorporation could be responsible for subnucleosome maturation. Due to our observation that subnucleosomes were enriched at H2A.Z sites upon *Smarca4* KD, we hypothesized that one role of esBAF in subnucleosome regulation could be through regulation of H2A.Z occupancy or incorporation at specific locations throughout the genome.

In mammals, H2A.Z is incorporated into nucleosomes by p400 and SRCAP via exchange of H2A/H2B dimers for H2A.Z/H2B dimers (Cai et al., 2005; Park et al., 2010; Ruhl et al., 2006; Wong et al., 2007), and these nucleosomes are enriched near specific genomic features, including enhancers and promoters (Mavrich et al., 2008b; Zilberman et al., 2008). H2A.Z nucleosomes play key roles in gene regulation, although the effect of H2A.Z incorporation on nucleosome stability and dynamics and their specific effects on transcription by RNAPII are controversial (Abbott et al., 2001; Jin and Felsenfeld, 2007; Park et al., 2004; Suto et al., 2000; Thambirajah et al., 2006; Thakar et al., 2010; Zhang et al., 2005).

We considered the possibility that esBAF regulates H2A.Z occupancy at enhancers and promoters either directly or indirectly. To test this possibility, we performed histone H2A.Z ChIP-seq in *EGFP*, *Mbd3*, and *Smarca4* KD cells. In *EGFP* KD cells, H2A.Z localization was similar to that observed previously in ESCs, confirming the specificity of our data sets (Figures 4A and S4A). We found that *Smarca4* KD led to decreased H2A.Z occupancy when one examines either all H2A.Z binding sites or TSSs in particular (Figures 4A and 4B). Although *Smarca4* KD also resulted in decreased H2A.Z occupancy at Lsd1 binding sites (Figure S4B), it had no effect at Pwp1 sites (Figure 4C) and modestly increased H2A.Z occupancy at MafK sites (Figure S4B), demonstrating that esBAF is required for H2A.Z occupancy at some, but not all, of its locations throughout the genome. Although we found no evidence that depletion of *Smarca4* alters p400 occupancy (Data S1A), *Smarca4* KD also

resulted in increased subnucleosome footprinting over p400 binding sites (Data S1C), consistent with the role of esBAF in regulation of H2A.Z localization.

Taken together, these data suggest that esBAF is required for H2A.Z occupancy at some locations. Upon *Smarca4* KD, H2A.Z is strongly depleted, and subnucleosomes partially replace nucleosomes at several regions where H2A.Z is normally enriched. Whether esBAF promotes H2A.Z incorporation by facilitating the functions of SWR1 family complexes, either directly or indirectly, or is required for the stability of H2A.Z containing nucleosomes remains unresolved (Figures 4D and 4E).

Conclusions

Chromatin-remodeling enzymes have been examined for their roles in regulation of nucleosome architecture in many cell types. However, their effects on intra-nucleosome architecture, as well as their roles in regulation of DNA-binding proteins, are not fully understood. Here, we showed that use of a single footprinting method, MNase-seq, combined with available factor occupancy data, uncovers dynamic regulation of factor binding and subnucleosome structures that can be confirmed by traditional approaches. We focused on two antagonistically functioning chromatin regulators, esBAF and Mbd3/NuRD, to gain a deeper understanding of their roles in modulating ESC chromatin architecture. However, this method should be broadly applicable as a screen for functional interactions between chromatin regulators and the gene-regulatory network in any organism/cell type where transcription-factor-binding data are available.

EXPERIMENTAL PROCEDURES

Cell Culture

E14 mouse ESCs were cultured as previously described (Chen et al., 2013). RNAi-mediated KD was performed with endoribonuclease-III-digested siRNAs (esiRNAs) as previously described (Fazzio et al., 2008) using Lipofectamine 2000 (Invitrogen). KDs were performed for 48 hr.

qRT-PCR

RNA was isolated using TRIzol reagent (Invitrogen) and used in a cDNA synthesis reaction with random hexamers (Promega). cDNA was used as a template in qPCR reactions using a FAST SYBR mix (KAPA Biosystems) on an Eppendorf Realplex with *Mbd3*-, *Smarca4*-, or *GAPDH*-specific primers (Hainer et al., 2015).

Western Blotting

Whole-cell lysates were extracted using WE16th buffer (25 mM Tris [pH 7.5], 125 mM NaCl, 2.5 mM EDTA, 0.05% SDS, 0.5% NP-40, and 10% w/v glycerol). Nuclear and cytoplasmic fractions were isolated using the NE-PER extraction kit (Thermo Scientific) following the manufacturer's instructions. Thirty micrograms of lysate were separated by SDS-PAGE, transferred to nitrocellulose (Life Sciences), and assayed by immunoblotting. The antibodies used to detect proteins were anti-Brg1 (1:1,000; Bethyl A300-813A), anti-Mbd3 (1:1,000; Bethyl A302-529A), anti-Klf4 (1:1,000; Millipore AB4138), anti-Pol II (1:1,000; Santa Cruz sc-899), anti-GAPDH (1:5,000; Cell Signaling 2118), and anti-actin (1:50,000; Sigma A1978).

MNase-Seq Analysis

We re-analyzed MNase-seq footprinting data for ESCs depleted of the indicated factors that were previously published (Hainer et al., 2015). See the Supplemental Experimental Procedures for details.

ChIP-Seq

ChIP experiments and single-end libraries of ChIP-enriched DNA were prepared as previously described (Chen et al., 2013). See the Supplemental Experimental Procedures for details.

ACCESSION NUMBERS

The accession number for the new genomic data sets reported in this paper is GEO: GSE68400.

SUPPLEMENTAL INFORMATION

Supplemental Information includes Supplemental Experimental Procedures, three figures, and one data file and can be found with this article online at http://dx.doi.org/10.1016/j.celrep.2015.08.071.

AUTHOR CONTRIBUTIONS

S.J.H. and T.G.F. designed all experiments. S.J.H. carried out all experiments and performed analyses of genomic data. S.J.H. and T.G.F. wrote the manuscript.

ACKNOWLEDGMENTS

We thank P. Chen, L. Ee, and K. McCannell for insightful discussions and critical reading of this manuscript. We thank H.-H. Ng from the Genome Institute of Singapore for the Klf4 antibody. This work was supported by the T32CA130807 training grant and a Leukemia and Lymphoma postdoctoral fellowship to S.J.H. and NIH HD072122 to T.G.F. T.G.F. was a Pew Scholar in the Biomedical Sciences and is a Leukemia and Lymphoma Society Scholar. The funders had no role in study design, data collection, analysis, decision to publish, or preparation of the manuscript. All deep sequencing was performed at the UMass Medical School Core facility on a HiSeq2000 supported by 1S10RR027052-01.

Received: May 11, 2015
Revised: August 1, 2015
Accepted: August 25, 2015
Published: September 24, 2015

REFERENCES

Abbott, D.W., Ivanova, V.S., Wang, X., Bonner, W.M., and Ausió, J. (2001). Characterization of the stability and folding of H2A.Z chromatin particles: implications for transcriptional activation. J. Biol. Chem. *276*, 41945–41949.

Almer, A., and Hörz, W. (1986). Nuclease hypersensitive regions with adjacent positioned nucleosomes mark the gene boundaries of the PHO5/PHO3 locus in yeast. EMBO J. *5*, 2681–2687.

Bartholomew, B. (2014). Regulating the chromatin landscape: structural and mechanistic perspectives. Annu. Rev. Biochem. *83*, 671–696.

Boeger, H., Griesenbeck, J., Strattan, J.S., and Kornberg, R.D. (2003). Nucleosomes unfold completely at a transcriptionally active promoter. Mol. Cell *11*, 1587–1598.

Cai, Y., Jin, J., Florens, L., Swanson, S.K., Kusch, T., Li, B., Workman, J.L., Washburn, M.P., Conaway, R.C., and Conaway, J.W. (2005). The mammalian YL1 protein is a shared subunit of the TRRAP/TIP60 histone acetyltransferase and SRCAP complexes. J. Biol. Chem. *280*, 13665–13670.

Carone, B.R., Hung, J.-H., Hainer, S.J., Chou, M.-T., Carone, D.M., Weng, Z., Fazzio, T.G., and Rando, O.J. (2014). High-resolution mapping of chromatin packaging in mouse embryonic stem cells and sperm. Dev. Cell *30*, 11–22.

Chen, X., Xu, H., Yuan, P., Fang, F., Huss, M., Vega, V.B., Wong, E., Orlov, Y.L., Zhang, W., Jiang, J., et al. (2008). Integration of external signaling pathways with the core transcriptional network in embryonic stem cells. Cell *133*, 1106–1117.

Chen, P.B., Hung, J.-H., Hickman, T.L., Coles, A.H., Carey, J.F., Weng, Z., Chu, F., and Fazzio, T.G. (2013). Hdac6 regulates Tip60-p400 function in stem cells. eLife *2*, e01557.

Denslow, S.A., and Wade, P.A. (2007). The human Mi-2/NuRD complex and gene regulation. Oncogene *26*, 5433–5438.

Fazzio, T.G., Huff, J.T., and Panning, B. (2008). An RNAi screen of chromatin proteins identifies Tip60-p400 as a regulator of embryonic stem cell identity. Cell *134*, 162–174.

Hainer, S.J., Gu, W., Carone, B.R., Landry, B.D., Rando, O.J., Mello, C.C., and Fazzio, T.G. (2015). Suppression of pervasive noncoding transcription in embryonic stem cells by esBAF. Genes Dev. *29*, 362–378.

Henikoff, J.G., Belsky, J.A., Krassovsky, K., MacAlpine, D.M., and Henikoff, S. (2011). Epigenome characterization at single base-pair resolution. Proc. Natl. Acad. Sci. USA *108*, 18318–18323.

Ho, L., Ronan, J.L., Wu, J., Staahl, B.T., Chen, L., Kuo, A., Lessard, J., Nesvizhskii, A.I., Ranish, J., and Crabtree, G.R. (2009a). An embryonic stem cell chromatin remodeling complex, esBAF, is essential for embryonic stem cell self-renewal and pluripotency. Proc. Natl. Acad. Sci. USA *106*, 5181–5186.

Ho, L., Jothi, R., Ronan, J.L., Cui, K., Zhao, K., and Crabtree, G.R. (2009b). An embryonic stem cell chromatin remodeling complex, esBAF, is an essential component of the core pluripotency transcriptional network. Proc. Natl. Acad. Sci. USA *106*, 5187–5191.

Ho, L., Miller, E.L., Ronan, J.L., Ho, W.Q., Jothi, R., and Crabtree, G.R. (2011). esBAF facilitates pluripotency by conditioning the genome for LIF/STAT3 signalling and by regulating polycomb function. Nat. Cell Biol. *13*, 903–913.

Jin, C., and Felsenfeld, G. (2007). Nucleosome stability mediated by histone variants H3.3 and H2A.Z. Genes Dev. *21*, 1519–1529.

Kaji, K., Caballero, I.M., MacLeod, R., Nichols, J., Wilson, V.A., and Hendrich, B. (2006). The NuRD component Mbd3 is required for pluripotency of embryonic stem cells. Nat. Cell Biol. *8*, 285–292.

Kaji, K., Nichols, J., and Hendrich, B. (2007). Mbd3, a component of the NuRD co-repressor complex, is required for development of pluripotent cells. Development *134*, 1123–1132.

Kent, N.A., Adams, S., Moorhouse, A., and Paszkiewicz, K. (2011). Chromatin particle spectrum analysis: a method for comparative chromatin structure analysis using paired-end mode next-generation DNA sequencing. Nucleic Acids Res. *39*, e26.

Kidder, B.L., Palmer, S., and Knott, J.G. (2009). SWI/SNF-Brg1 regulates self-renewal and occupies core pluripotency-related genes in embryonic stem cells. Stem Cells *27*, 317–328.

Kim, M.O., Kim, S.-H., Cho, Y.-Y., Nadas, J., Jeong, C.-H., Yao, K., Kim, D.J., Yu, D.-H., Keum, Y.-S., Lee, K.-Y., et al. (2012). ERK1 and ERK2 regulate embryonic stem cell self-renewal through phosphorylation of Klf4. Nat. Struct. Mol. Biol. *19*, 283–290.

Li, Z., Gadue, P., Chen, K., Jiao, Y., Tuteja, G., Schug, J., Li, W., and Kaestner, K.H. (2012). Foxa2 and H2A.Z mediate nucleosome depletion during embryonic stem cell differentiation. Cell *151*, 1608–1616.

Luger, K., Mäder, A.W., Richmond, R.K., Sargent, D.F., and Richmond, T.J. (1997). Crystal structure of the nucleosome core particle at 2.8 A resolution. Nature *389*, 251–260.

Margueron, R., and Reinberg, D. (2011). The Polycomb complex PRC2 and its mark in life. Nature *469*, 343–349.

Mavrich, T.N., Ioshikhes, I.P., Venters, B.J., Jiang, C., Tomsho, L.P., Qi, J., Schuster, S.C., Albert, I., and Pugh, B.F. (2008a). A barrier nucleosome model for statistical positioning of nucleosomes throughout the yeast genome. Genome Res. *18*, 1073–1083.

Mavrich, T.N., Jiang, C., Ioshikhes, I.P., Li, X., Venters, B.J., Zanton, S.J., Tomsho, L.P., Qi, J., Glaser, R.L., Schuster, S.C., et al. (2008b). Nucleosome organization in the Drosophila genome. Nature *453*, 358–362.

Novershtern, N., and Hanna, J.H. (2011). esBAF safeguards Stat3 binding to maintain pluripotency. Nat. Cell Biol. *13*, 886–888.

Park, Y.-J., Dyer, P.N., Tremethick, D.J., and Luger, K. (2004). A new fluorescence resonance energy transfer approach demonstrates that the histone variant H2AZ stabilizes the histone octamer within the nucleosome. J. Biol. Chem. *279*, 24274–24282.

Park, J.H., Sun, X.-J., and Roeder, R.G. (2010). The SANT domain of p400 ATPase represses acetyltransferase activity and coactivator function of TIP60 in basal p21 gene expression. Mol. Cell. Biol. *30*, 2750–2761.

Pasini, D., Malatesta, M., Jung, H.R., Walfridsson, J., Willer, A., Olsson, L., Skotte, J., Wutz, A., Porse, B., Jensen, O.N., and Helin, K. (2010). Characterization of an antagonistic switch between histone H3 lysine 27 methylation and acetylation in the transcriptional regulation of Polycomb group target genes. Nucleic Acids Res. *38*, 4958–4969.

Percharde, M., Lavial, F., Ng, J.-H., Kumar, V., Tomaz, R.A., Martin, N., Yeo, J.-C., Gil, J., Prabhakar, S., Ng, H.-H., et al. (2012). Ncoa3 functions as an essential Esrrb coactivator to sustain embryonic stem cell self-renewal and reprogramming. Genes Dev. *26*, 2286–2298.

Racki, L.R., and Narlikar, G.J. (2008). ATP-dependent chromatin remodeling enzymes: two heads are not better, just different. Curr. Opin. Genet. Dev. *18*, 137–144.

Reynolds, N., Salmon-Divon, M., Dvinge, H., Hynes-Allen, A., Balasooriya, G., Leaford, D., Behrens, A., Bertone, P., and Hendrich, B. (2012). NuRD-mediated deacetylation of H3K27 facilitates recruitment of Polycomb Repressive Complex 2 to direct gene repression. EMBO J. *31*, 593–605.

Rhee, H.S., Bataille, A.R., Zhang, L., and Pugh, B.F. (2014). Subnucleosomal structures and nucleosome asymmetry across a genome. Cell *159*, 1377–1388.

Ruhl, D.D., Jin, J., Cai, Y., Swanson, S., Florens, L., Washburn, M.P., Conaway, R.C., Conaway, J.W., and Chrivia, J.C. (2006). Purification of a human SRCAP complex that remodels chromatin by incorporating the histone variant H2A.Z into nucleosomes. Biochemistry *45*, 5671–5677.

Schaniel, C., Ang, Y.-S., Ratnakumar, K., Cormier, C., James, T., Bernstein, E., Lemischka, I.R., and Paddison, P.J. (2009). Smarcc1/Baf155 couples self-renewal gene repression with changes in chromatin structure in mouse embryonic stem cells. Stem Cells *27*, 2979–2991.

Schones, D.E., Cui, K., Cuddapah, S., Roh, T.-Y., Barski, A., Wang, Z., Wei, G., and Zhao, K. (2008). Dynamic regulation of nucleosome positioning in the human genome. Cell *132*, 887–898.

Schuh, R., Aicher, W., Gaul, U., Côté, S., Preiss, A., Maier, D., Seifert, E., Nauber, U., Schröder, C., Kemler, R., et al. (1986). A conserved family of nuclear proteins containing structural elements of the finger protein encoded by Krüppel, a Drosophila segmentation gene. Cell *47*, 1025–1032.

Shen, J., Jia, W., Yu, Y., Chen, J., Cao, X., Du, Y., Zhang, X., Zhu, S., Chen, W., Xi, J., et al. (2015). Pwp1 is required for the differentiation potential of mouse embryonic stem cells through regulating Stat3 signaling. Stem Cells *33*, 661–673.

Shi, Y., Lan, F., Matson, C., Mulligan, P., Whetstine, J.R., Cole, P.A., Casero, R.A., and Shi, Y. (2004). Histone demethylation mediated by the nuclear amine oxidase homolog LSD1. Cell *119*, 941–953.

Simon, J.A., and Kingston, R.E. (2009). Mechanisms of polycomb gene silencing: knowns and unknowns. Nat. Rev. Mol. Cell Biol. *10*, 697–708.

Suto, R.K., Clarkson, M.J., Tremethick, D.J., and Luger, K. (2000). Crystal structure of a nucleosome core particle containing the variant histone H2A.Z. Nat. Struct. Biol. *7*, 1121–1124.

Takahashi, K., and Yamanaka, S. (2006). Induction of pluripotent stem cells from mouse embryonic and adult fibroblast cultures by defined factors. Cell *126*, 663–676.

Teif, V.B., Vainshtein, Y., Caudron-Herger, M., Mallm, J.-P., Marth, C., Höfer, T., and Rippe, K. (2012). Genome-wide nucleosome positioning during embryonic stem cell development. Nat. Struct. Mol. Biol. *19*, 1185–1192.

Thakar, A., Gupta, P., McAllister, W.T., and Zlatanova, J. (2010). Histone variant H2A.Z inhibits transcription in reconstituted nucleosomes. Biochemistry *49*, 4018–4026.

Thambirajah, A.A., Dryhurst, D., Ishibashi, T., Li, A., Maffey, A.H., and Ausió, J. (2006). H2A.Z stabilizes chromatin in a way that is dependent on core histone acetylation. J. Biol. Chem. *281*, 20036–20044.

Valouev, A., Johnson, S.M., Boyd, S.D., Smith, C.L., Fire, A.Z., and Sidow, A. (2011). Determinants of nucleosome organization in primary human cells. Nature *474*, 516–520.

Wang, H., Wang, L., Erdjument-Bromage, H., Vidal, M., Tempst, P., Jones, R.S., and Zhang, Y. (2004). Role of histone H2A ubiquitination in Polycomb silencing. Nature *431*, 873–878.

Weiner, A., Hughes, A., Yassour, M., Rando, O.J., and Friedman, N. (2010). High-resolution nucleosome mapping reveals transcription-dependent promoter packaging. Genome Res. *20*, 90–100.

Weintraub, H., Palter, K., and Van Lente, F. (1975). Histones H2a, H2b, H3, and H4 form a tetrameric complex in solutions of high salt. Cell *6*, 85–110.

Wong, M.M., Cox, L.K., and Chrivia, J.C. (2007). The chromatin remodeling protein, SRCAP, is critical for deposition of the histone variant H2A.Z at promoters. J. Biol. Chem. *282*, 26132–26139.

Yildirim, O., Li, R., Hung, J.-H., Chen, P.B., Dong, X., Ee, L.-S., Weng, Z., Rando, O.J., and Fazzio, T.G. (2011). Mbd3/NURD complex regulates expression of 5-hydroxymethylcytosine marked genes in embryonic stem cells. Cell *147*, 1498–1510.

Yuan, G.-C., Liu, Y.-J., Dion, M.F., Slack, M.D., Wu, L.F., Altschuler, S.J., and Rando, O.J. (2005). Genome-scale identification of nucleosome positions in S. cerevisiae. Science *309*, 626–630.

Zhang, H., Roberts, D.N., and Cairns, B.R. (2005). Genome-wide dynamics of Htz1, a histone H2A variant that poises repressed/basal promoters for activation through histone loss. Cell *123*, 219–231.

Zhang, Z., Jones, A., Sun, C.W., Li, C., Chang, C.W., Joo, H.Y., Dai, Q., Mysliwiec, M.R., Wu, L.C., Guo, Y., et al. (2011). PRC2 complexes with JARID2, MTF2, and esPRC2p48 in ES cells to modulate ES cell pluripotency and somatic cell reprogramming. Stem Cells *29*, 229–240.

Zilberman, D., Coleman-Derr, D., Ballinger, T., and Henikoff, S. (2008). Histone H2A.Z and DNA methylation are mutually antagonistic chromatin marks. Nature *456*, 125–129.

Cell Reports

Supplemental Information

Regulation of Nucleosome Architecture and Factor Binding Revealed by Nuclease Footprinting of the ESC Genome

Sarah J. Hainer and Thomas G. Fazzio

SUPPLEMENTAL INFORMATION

SUPPLEMENTAL EXPERIMENTAL PROCEDURES

Analysis of MNase-seq footprints

We re-analyzed MNase-seq footprinting data for ESCs depleted of the indicated factors that were previously published (Hainer et al., 2015) (GEO: GSE57170). Libraries were constructed from total MNase digested DNA (not size selected) and were then selected and purified with Agencourt Ampure beads, as previously described (Carone et al., 2014; Henikoff et al., 2011), to provide a range of DNA footprints up to ~200 bp. To increase the signal-noise ratio of MNase footprints, we obtained additional coverage of the same libraries on an Illumina HiSeq2000 using paired-end sequencing (100 bp) at the UMass Medical School deep sequencing core facility.

Data analysis

Paired-end reads were collapsed and adapter sequences were removed from fastq files. Reads were mapped to the mouse mm9 genome using Bowtie2, and only uniquely mapped reads with zero, one, or two mismatches were used. The read size distribution was determined for each library, and reads were sorted for small read size fragments (≤80 bp), subnucleosome size fragments (100-130 bp), and nucleosome size fragments (135-165 bp). To calculate occupancy around factor binding sites, seqMINER (Ye et al., 2011) was used to sum reads 2000 bp upstream and downstream of the factor binding site sequences obtained from

previously performed ChIP-seq experiments, binned in 20 bp intervals, and normalized to the average, genome-wide coverage. TSS reference sites were used based on mm9 TSS coordinates. Factor binding site sequences were called from: Brg1 (GEO:GSE27708), Mbd3 (GEO:GSE31690), Mtf2 (GEO:GSE19708), Pwp1 (GEO:GSE59389), Ezh2 (ENCODE), Suz12 (GEO:GSE11724), Esrrb (GEO:GSE11431), Ring1B (GEO:GSE52619), NcoA3 (GEO:GSE40193), MafK (GEO:GSE49847), MacroH2A1 (GEO:GSE35087), Yy1 (GEO:GSE25197), Nanog (GEO:GSE11724), Oct4 (GEO:GSE11724), H3.3 (GEO:GSE16893), H2A.Z (GEO:GSE34483), Nipbl (GEO:GSE22562), p300 (GEO:GSE49847), Sox2 (GEO:GSE11724), SetDB1 (GEO:GSE18371), Znf384 (GEO:GSM1003807), Hcfc1 (GEO:GSE49847), Zc3h11A (GEO:GSE49847), Lsd1 (GEO:GSE18515), Klf4 (GEO:GSE11431), Tcf3 (GEO:GSE11724), Med1 (GEO:GSE22562), Med12 (GEO:GSE22562), Smc1 (GEO:GSE22562), Smc3 (GEO:GSE22562), and p400 (GEO:GSE42209).

ChIP-seq

ChIP experiments were performed as previously described (Hainer et al., 2015). Cells from RNAi-mediated KD were fixed, washed with ice-cold PBS, and pelleted. Cell pellets were lysed through sonication in a Bioruptor (UCD-200), and supernatants were saved. 30 µL of chromatin was stored overnight at 4°C for input samples while the remainder of the chromatin was combined with antibody coupled protein A magnetic beads (NEB) and incubated at 4°C overnight with constant rotation. H3 antibody (abcam, ab1791), H2A.Z antibody (abcam, ab4174), or Klf4 antibody (kind gift from Huck Hui Ng from the Genome Institute

of Singapore, (Chen et al., 2008)) coupled protein A magnetic beads (NEB) were blocked with 5 mg/mL BSA overnight at 4°C, prior to incubation with sheared chromatin. Magnetic beads were washed, and material was eluted at 65°C on a thermomixer. Eluted material was combined to a new microfuge tube and incubated at 65°C overnight to reverse crosslinking. Input DNA was diluted with 170 µL elution buffer and treated similarly. Samples were treated with RNaseA/T1 (Ambion) and proteinase K (Ambion) and then PCI extracted. Ethanol precipitated ChIP-enriched DNA was then used for library construction.

Library construction

Single-end libraries of ChIP-enriched DNA were prepared as described previously (Chen et al., 2013). Samples were end-repaired, A-tailed, and adaptor-ligated with DNA purification over a column between each step. DNA was PCR amplified with KAPA HiFi polymerase using 16 cycles of PCR. The library was size-selected on a 1% agarose gel, its concentration determined using a NanoDrop (Thermo), and the integrity was confirmed by sequencing ~10 fragments from each library. Libraries were sequenced on an Illumina HiSeq2000 using single-end sequencing (50 bp) at the UMass Medical School deep sequencing core facility.

Data Analysis

Single-end fastq reads were collapsed, adapter sequences were removed, and reads were mapped to the mm9 genome using bowtie, allowing one mismatch. Aligned reads were processed in HOMER (Heinz et al., 2010) by using the "annotatePeaks" command to make 20 bp bins over regions of interest and sum

the reads within each window. H3 ChIP-seq experiments were aligned over the following datasets: H2A.Z (GEO:GSE34483), Pwp1 (GEO:GSE59389), NcoA3 (GEO:GSE40193), Esrrb (GEO:GSE11431), Lsd1 (GEO:GSE18515), MafK (GEO:GSE49847), Ring1B (GEO:GSE52619), Ezh2 (ENCODE), and TSS reference sites based on mm9 TSS coordinates. H2A.Z ChIP-seq experiments were aligned over the following datasets: H2A.Z (GEO:GSE34483 (Figure 4A) and GEO:GSE39237 (Figure S3)), Pwp1 (GEO:GSE59389), Lsd1 (GEO:GSE18515), MafK (GEO:GSE49847) and TSS reference sites based on mm9 TSS coordinates.

SUPPLEMENTAL FIGURES

Supplemental Figure 1, related to Figure 1. Confirmation of efficient *Mbd3* KD and *Smarca4* KD.

(A-D) Efficient KD of *Mbd3* **(A-B)** and *Smarca4* **(C-D)** in ESCs confirmed by random primed RT-qPCR with expression levels normalized to *GAPDH* and shown relative to *EGFP* KD **(A,C)** and through Western blotting, where actin serves as a loading control **(B,D)** Asterisk (*) indicates a non-specific band. **(E)** MNase digestion on *EGFP* KD, *Mbd3* KD, and *Smarca4* KD. Asterisk (*) indicates samples used in MNase-seq experiment.

Supplemental Figure 2, related to Figures 2 and 3. esBAF regulates histone H3 occupancy over Ezh2 and Ring1B binding sites.

Aggregation plots of histone H3 ChIP-seq over Ezh2 and Ring1B binding sites in *EGFP*, *Mbd3*, and *Smarca4* KD ESCs. Asterisks (*, **) indicate p-values as described in Figure 1.

Supplemental Figure 3, related to Figure 4. Brg1 is required for H2A.Z occupancy at a subset of locations.

(A) Heatmaps of H2A.Z occupancy over published H2A.Z binding sites in *EGFP* (left) and *Smarca4* (right) KD ESCs. Binding sites were taken from (GEO:GSE39237). Occupancy is indicated as $\log_2$(normalized reads). **(B)** Aggregation plots of histone H2A.Z ChIP-seq over a subset of transcription factor binding sites +/− 2 kb of *EGFP* KD, *Mbd3* KD, and *Smarca4* KD ESCs. Asterisks (*, **) indicate p-values (<0.05, <0.01) reflecting statistical significance of changes in H2A.Z occupancy over the factor peak in *Mbd3* relative to *EGFP* KD (red) or *Smarca4* relative to *EGFP* KD (green).

Supplemental Data 1, related to Figures 1-3. Small reads, nucleosome size reads, and subnucleosomes size reads from MNase-seq reveal unique patterns in *Mbd3* KD and *Smarca4* KD ESCs.

(A-C) Aggregation plots of relative factor occupancy obtained from small read size fragments (≤80 bp, **A**), mononucleosome size fragments (135-165 bp, **B**), and sub-mononucleosome size fragments (100-130 bp, **C**) of MNase-seq data upon *EGFP* KD, *Mbd3* KD, or *Smarca4* KD averaged over various factor binding sites +/− 2 kb in ESCs. Binding sites were called from previously published ChIP-

seq datasets (see Supplemental Experimental Procedures). Asterisks (*, **) indicate p-values (<0.05, <0.01) reflecting statistical significance of changes in reads of each size class over the factor peak in *Mbd3* relative to *EGFP* KD (red) or *Smarca4* relative to *EGFP* KD (green).

SUPPLEMENTAL REFERENCES

Carone, B.R., Hung, J.-H., Hainer, S.J., Chou, M.-T., Carone, D.M., Weng, Z., Fazzio, T.G., and Rando, O.J. (2014). High-Resolution Mapping of Chromatin Packaging in Mouse Embryonic Stem Cells and Sperm. Developmental Cell *30*, 11–22.

Chen, P.B., Hung, J.-H., Hickman, T.L., Coles, A.H., Carey, J.F., Weng, Z., Chu, F., and Fazzio, T.G. (2013). Hdac6 regulates Tip60-p400 function in stem cells. eLife *2*, e01557.

Chen, X., Xu, H., Yuan, P., Fang, F., Huss, M., Vega, V.B., Wong, E., Orlov, Y.L., Zhang, W., Jiang, J. et al. (2008). Integration of external signaling pathways with the core transcriptional network in embryonic stem cells. Cell *133,* 1106-1117.

Hainer, S.J., Gu, W., Carone, B.R., Landry, B.D., Rando, O.J., Mello, C.C., and Fazzio, T.G. (2015). Suppression of pervasive noncoding transcription in embryonic stem cells by esBAF. Genes Dev. *29*, 362–378.

Heinz, S., Benner, C., Spann, N., Bertolino, E., Lin, Y.C., Laslo, P., Cheng, J.X., Murre, C., Singh, H., Glass, C.K. (2010). Simple Combinations of Lineage-Determining Transcription Factors Prime cis-Regulatory Elements Required for Macrophage and B Cell Identities. Molecular Cell *38*, 576-589.

Henikoff, J.G., Belsky, J.A., Krassovsky, K., MacAlpine, D.M., and Henikoff, S. (2011). Epigenome characterization at single base-pair resolution. PNAS *108*, 18318–18323.

Ye, T., Krebs, A.R., Choukrallah, M.A., and Keime, C. (2011). seqMINER: an integrated ChIP-seq data interpretation platform. Nucleic Acids Research *39*, e35–e44.

Supplemental Figure 1

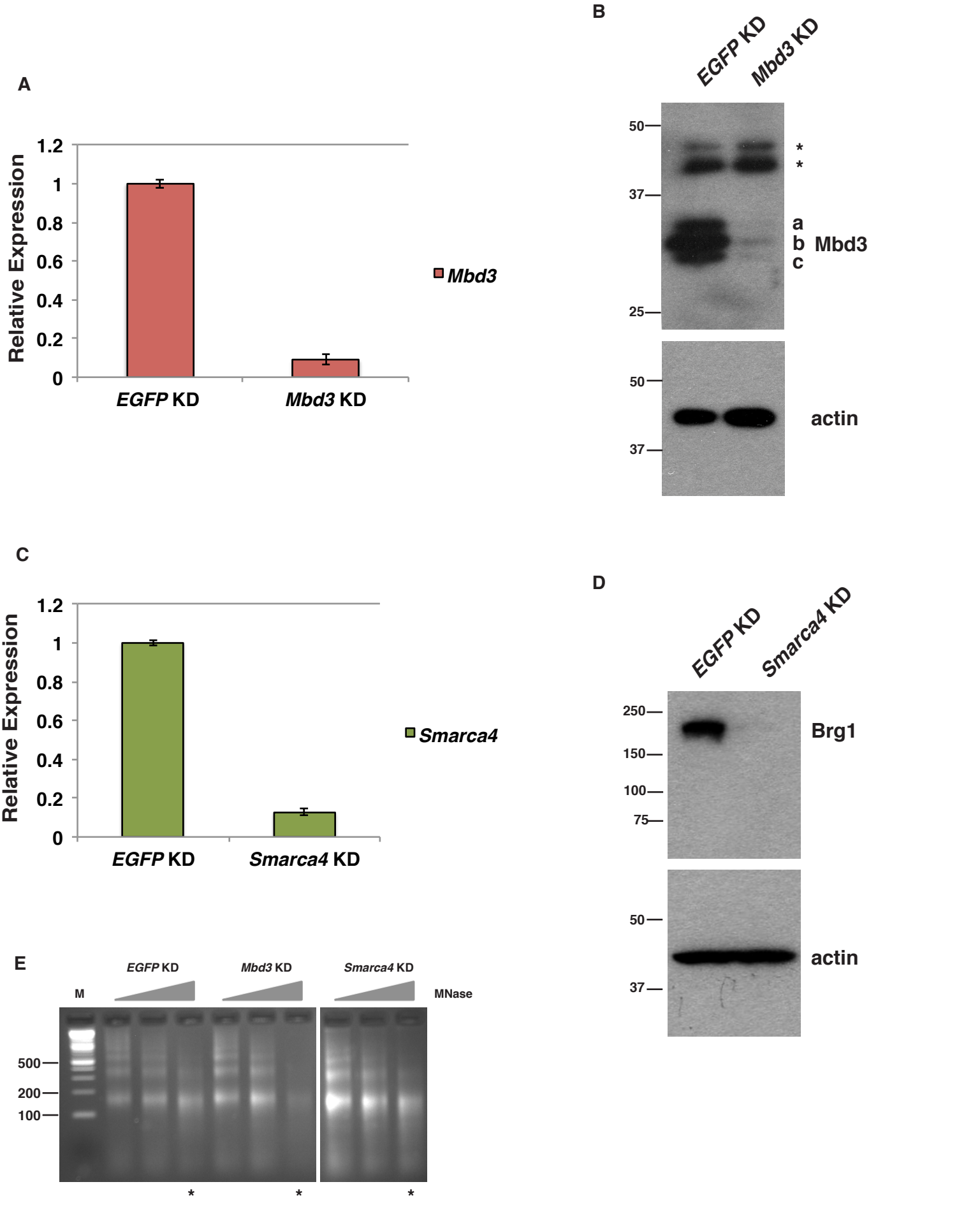

Supplemental Figure 2

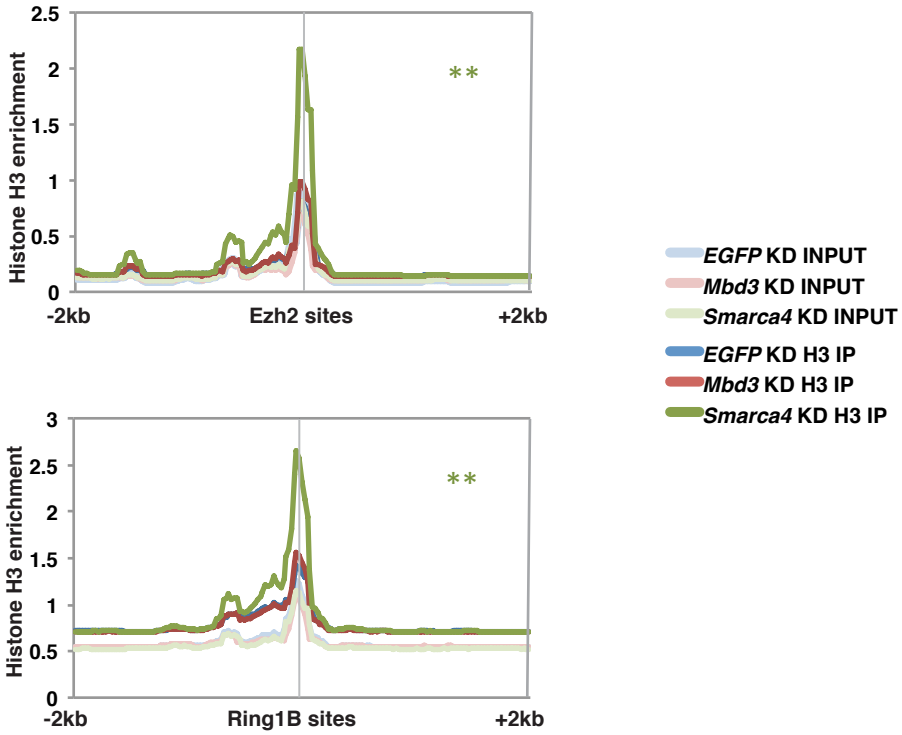

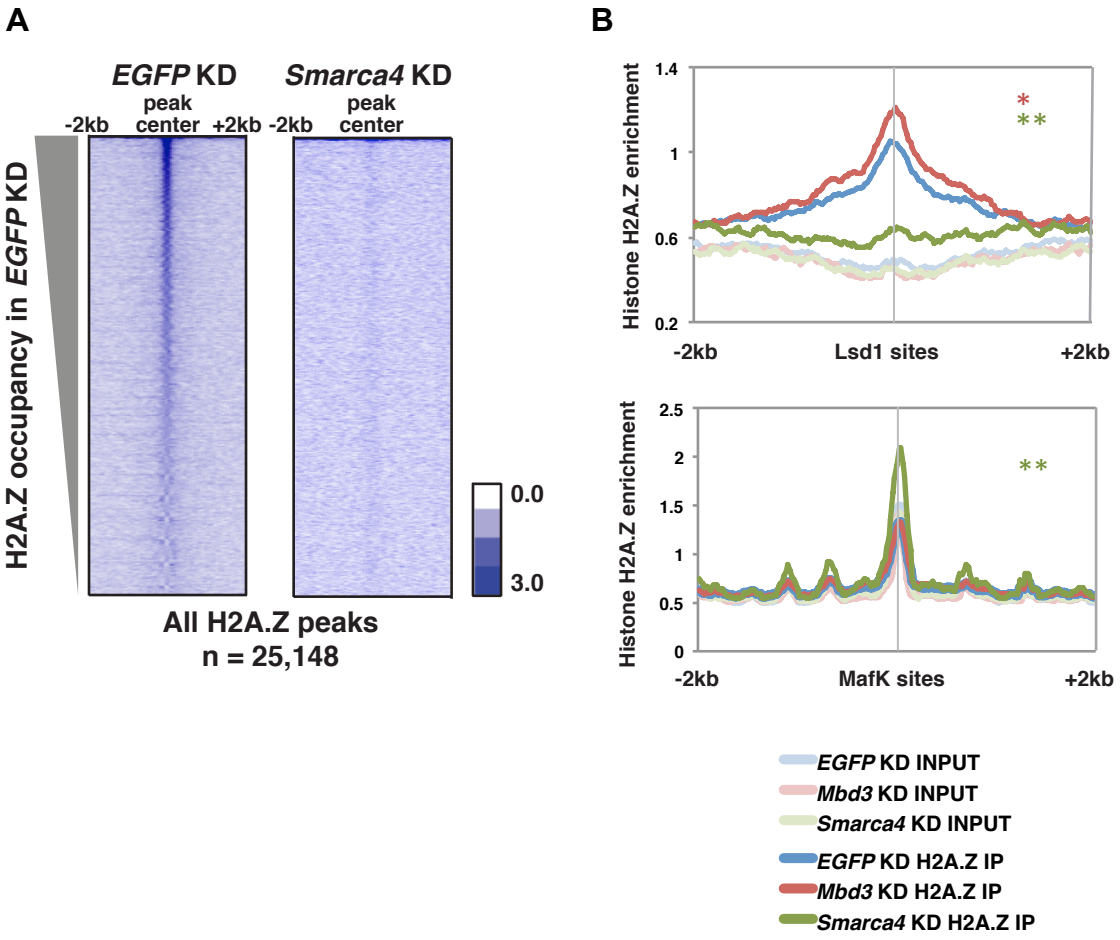
A
EGFP KD
Smarca4 KD
peak center
-2kb
+2kb
H2A.Z occupancy in EGFP KD
0.0
3.0
All H2A.Z peaks
n = 25,148
B
Histone H2A.Z enrichment
1.4
1
0.6
0.2
*
**
-2kb
Lsd1 sites
+2kb
2.5
2
1.5
1
0.5
0
MafK sites
EGFP KD INPUT
Mbd3 KD INPUT
Smarca4 KD INPUT
EGFP KD H2A.Z IP
Mbd3 KD H2A.Z IP
Smarca4 KD H2A.Z IP